

Supplementary Information

Bismuth oxyiodide microflowers-derived catalysts for efficient CO₂ electroreduction in a wide negative potential region

Peng Fei Liu,^{a†} Meng Yang Zu,^{a†} Li Rong Zheng,^b Hua Gui Yang^{a*}

^a Key Laboratory for Ultrafine Materials of Ministry of Education, School of Materials Science and Engineering, Shanghai Engineering Research Center of Hierarchical Nanomaterials, East China University of Science and Technology, Shanghai 200237, China.

^b Institute of High Energy Physics, Chinese Academy of Sciences, Beijing 100049, China.

† These authors contributed equally to this work.

* Correspondence and requests for materials should be addressed to H.G.Y. (email: hgyang@ecust.edu.cn).

Experimental sections

Materials: Analytical grade bismuth(III) nitrate pentahydrate ($\text{Bi}(\text{NO}_3)_3 \cdot 5\text{H}_2\text{O}$) was purchased from Alfa Aesar, and potassium iodide (KI) was brought from Shanghai Tianlian Chemical Technology Co. Ltd. Iso-propyl alcohol, urea ($\text{CO}(\text{NH}_2)_2$) and potassium bicarbonate (KHCO_3) were obtained from Shanghai Chemical Reagent Co. Ltd. Ethylene glycol and absolute ethanol were obtained from Shanghai Lingfeng Chemical Reagent Co. Ltd. Commercial Bi powders (325 mesh) were purchased from Macklin. Nafion[®] solution (5 wt%) was purchased from Sigma-Aldrich. Carbon papers were brought from Toray. All chemicals were used without further purification. Deionized (DI) water used in our experiments was supplied by Milli-Q System (Millipore, Billerica, MA).

Synthesis of BiOI: In the typical synthesis of BiOI microflowers, 0.498 g KI was dissolved in 40 mL ethylene glycol, and then 1.445g $\text{Bi}(\text{NO}_3)_3 \cdot 5\text{H}_2\text{O}$ was slowly added into the above solution under continuously stirring for 0.5 h to form a homogenous solution. The obtained solution was transferred into a 50 mL Teflon-lined stainless steel autoclave, and then sealed and heated at 160 °C for 12 h. After the hydrothermal reaction, the samples were completely washed with DI water for 3 times and dried in a vacuum oven of 60 °C for 12 h to obtain the final BiOI products.

Synthesis of $\text{Bi}_2\text{O}_2\text{CO}_3$: In the typical synthesis of $\text{Bi}_2\text{O}_2\text{CO}_3$ nanosheets, 0.243g $\text{Bi}(\text{NO}_3)_3 \cdot 5\text{H}_2\text{O}$ was dissolved in 10 mL DI water. Then, the solution of 1.502 g urea dissolved in 10 mL ethanol was slowly added into the above solution under continuously stirring for 0.5 h. The mixed solution was placed in the oil bath under 90 °C for 4 h with stirring. The samples were washed with DI water and ethanol each for 2 times and the products were dried in a vacuum oven of 60 °C for 12 h to obtain the final $\text{Bi}_2\text{O}_2\text{CO}_3$ products.

Preparation of catalytic electrodes: All the samples were drop coated onto the carbon paper substrate (with 1 cm × 2 cm in total, and catalytic exposure areas of 1 cm × 1 cm) as catalytic electrodes for the electrochemical measurements. Carbon papers were cleaned with concentrated HNO_3 through refluxing under 100 °C for 6 h, then washed with plenty of deionized water and dried for further measurements. The electrodes were manufactured as follows: the mixture of catalyst (10 mg) and carbon powder (10 mg) suspended in 2-propanol solution (920 μL) containing Nafion[®] solution (80 μL) by sonication dispersing. After sonication for 30 min, the slurry (200 μL) was dropped onto carbon paper and formed a 1 cm × 1 cm uniform coating, then dried naturally

under ambient temperature for overnight. The final loading quantity of catalysts is about 2.0 mg cm^{-2} .

Electrochemical measurements: Electrochemical measurements were performed by using a Model CHI 660E electrochemical station in a two-compartment electrochemical cell under ambient temperature, and Nafion 115, which is a proton exchange membrane, was used to separate the catholyte and the anolyte. Ar- or CO_2 -saturated KHCO_3 (0.5 M) aqueous solution acts as the electrolyte for testing the performance of catalysts. Bi based electrocatalysts decorated carbon papers, Ag/AgCl (3.5 M KCl) and gauze platinum were used as the working electrode, the reference electrode and the counter electrode, respectively. All the applied potentials have been transferred to reversible hydrogen electrode (RHE) potential based on the equation: $E_{\text{RHE}} = E_{\text{Ag/AgCl}} + 0.205 \text{ V} + 0.059 \times \text{pH}$. The gas flux was controlled precisely at 5 sccm with mass flow controller (Alicat Scientific, USA, LK2).

Products analysis: The CO_2 reduction reaction was measured by using chronoamperometric tests at each fixed cathodic potential. Online gas chromatography (RAMIIN, GC2060) was connected with the reaction cell to quantify the gas products, in which thermal conductivity detector (TCD, for H_2) and a flame ionization detector (FIF, for CO and other gaseous hydrocarbons) were equipped.

The Faradaic efficiency (FE) for formation of CO or H_2 was calculated as below:

$$FE = 2\chi \times p \times G \times F / (I \times R \times T)$$

Where χ (vol%) is the volume fractions of CO and H_2 in the exhaust gas, I (A) is the steady-state total current, $G = 5 \text{ mL min}^{-1}$ is the CO_2 flow rate, $p = 1.013 \times 10^5 \text{ Pa}$, $T = 273.15 \text{ K}$, $F = 96485 \text{ C mol}^{-1}$, $R = 8.3145 \text{ J mol}^{-1} \text{ K}^{-1}$.

Liquid product of HCOO^- was quantified using ^1H nuclear magnetic resonance (NMR). For analysis, a 0.5 mL aliquot of the electrolyte was mixed with 0.1 mL D_2O (with TMSP as the internal standard). The Faradaic efficiency for formation of HCOO^- was calculated as below:

$$FE = 2F \times n_{\text{HCOO}^-} / (I \times t)$$

Characterizations: The crystal structure of the samples was examined by X-ray diffraction (XRD, D/max2550V). The morphology of the samples was determined by scanning electron microscopy (Hitachi S4800) and transmission electron microscopy (TEM, JEM 2100, 200 kV). Chemical valence states were analyzed by X-ray photoelectron spectroscopy (XPS, Thermo Escalab 250) with Al $K\alpha$ X-ray beam (1486.6 eV), and all binding energies were calibrated using the C 1s peak at 284.8 eV as the reference. XAFS spectra at the Bi L_3 edge were performed on the 1W1B beamline

station of the Beijing Synchrotron Radiation Facility (BSRF), China. Commercial Bi powders were used as the reference. Liquid products were analyzed by NMR (Bruker AVANCEIII) spectroscopy with water suppression using a pre-saturation method.

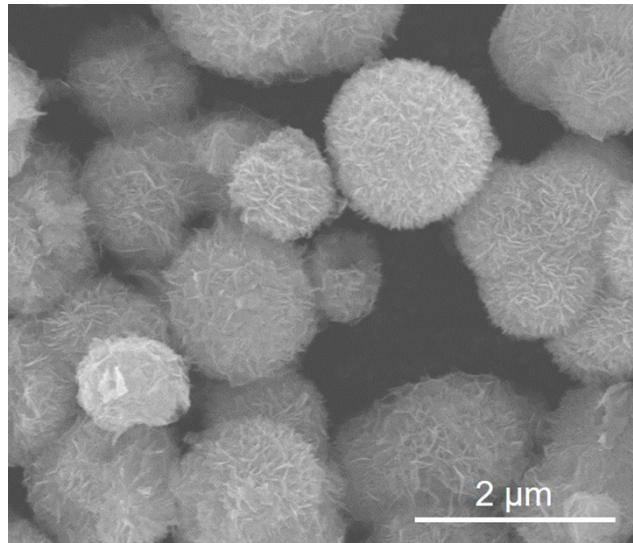


Fig. S1 SEM image of the pristine BiOI microflowers.

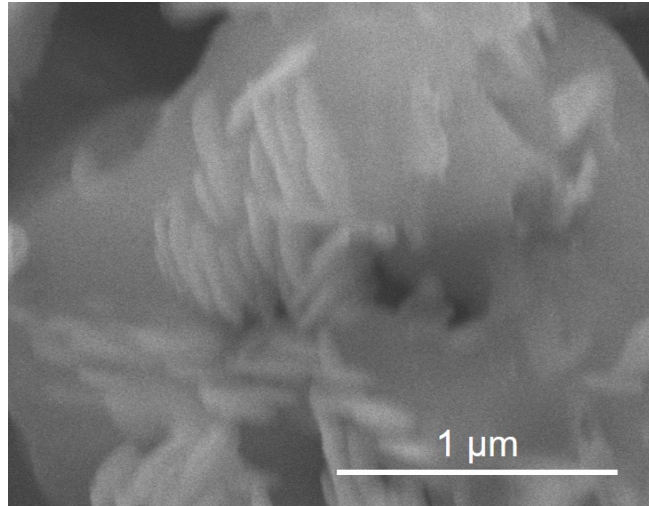


Fig. S2 SEM image of BiOI samples collected after CO₂RR process.

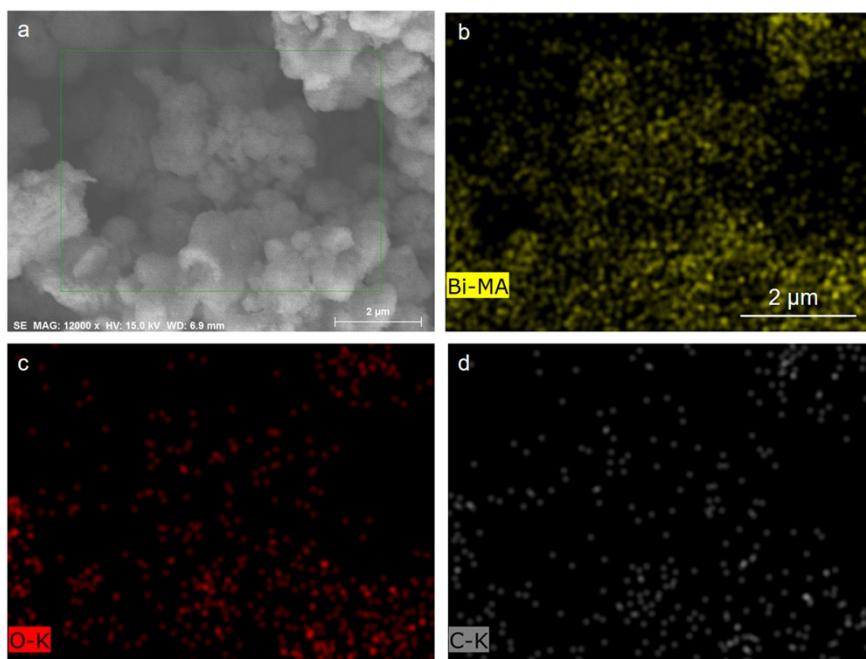


Fig. S3 (a) SEM image of P-BiOI collected after reduction at the potential of -1.00 V for 2 hours on the glassy carbon electrode without carbon additives and corresponding mapping images of (b) Bi, (c) O and (d) C elements, respectively, indicating the main component of metallic Bi elements in the whole region

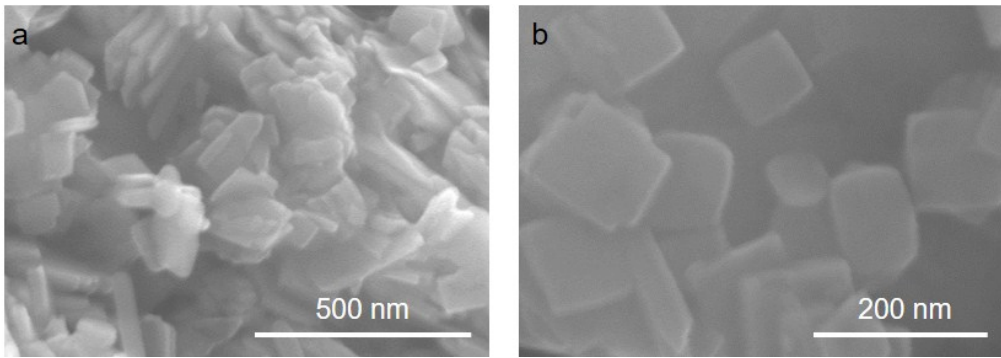


Fig. S4 (a, b) SEM images of typical $\text{Bi}_2\text{O}_2\text{CO}_3$ nanosheets at different magnifications.

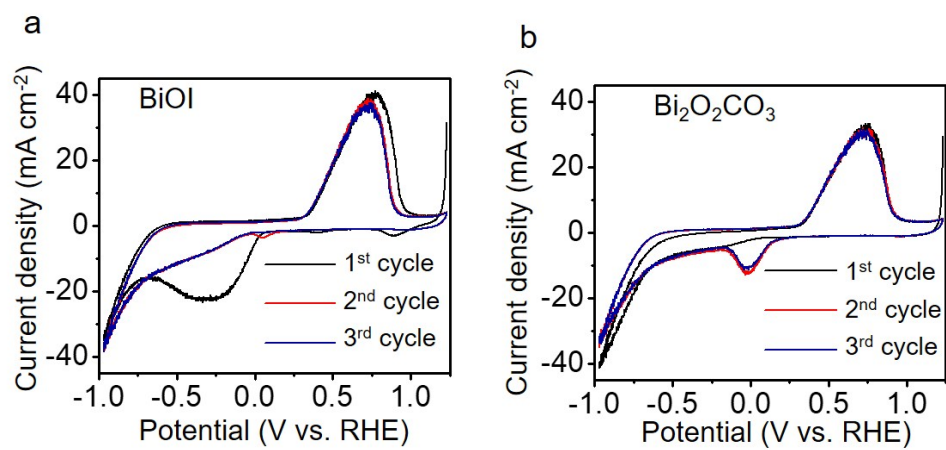


Fig. S5 Cyclic voltammetric curves of (a) BiOI and (b) Bi₂O₂CO₃ with three continuous scans. XPS spectra.

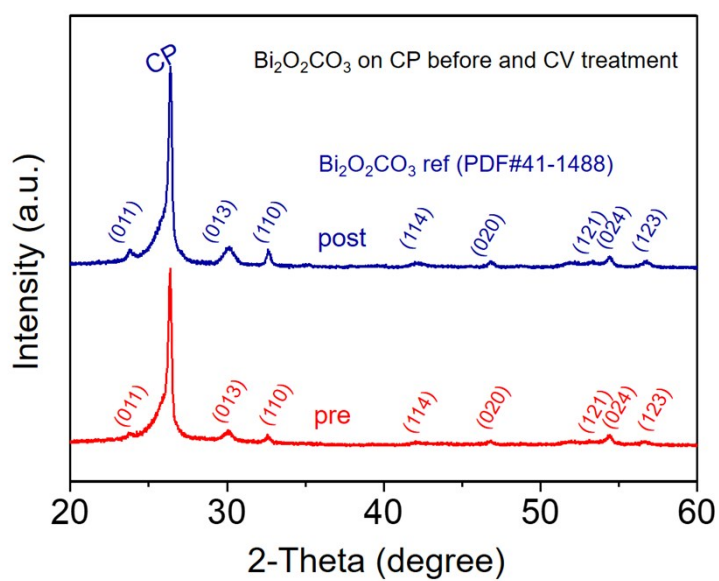


Fig. S6 XRD patterns of Bi₂O₂CO₃ samples decorated carbon paper electrode before and after CO₂RR test.

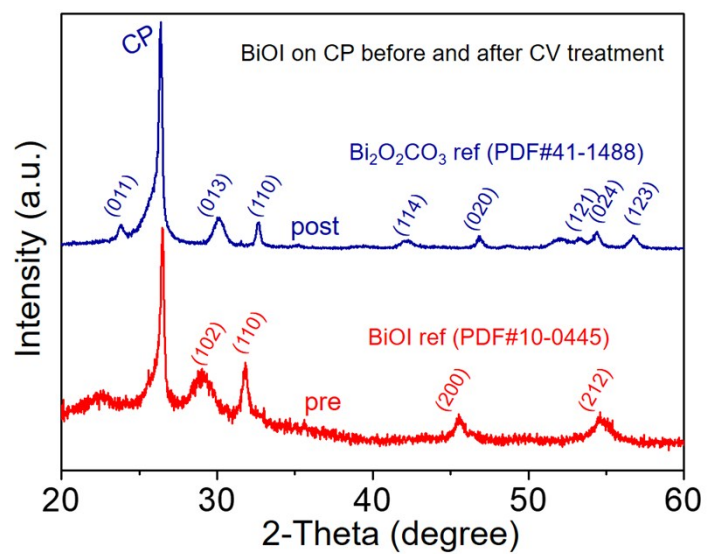


Fig. S7 XRD patterns of BiOI samples decorated carbon paper electrode before and after CO_2RR test.

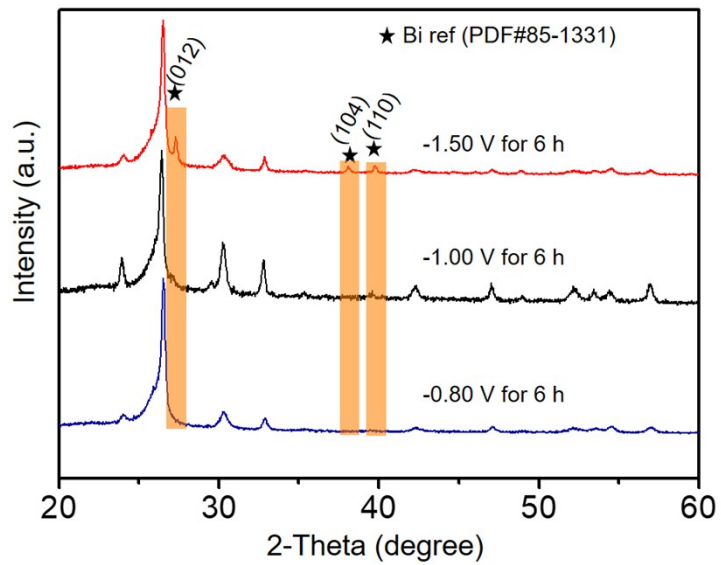


Fig. S8 XRD patterns of BiOI samples which were biased at the different cathodic potentials for 6 h.

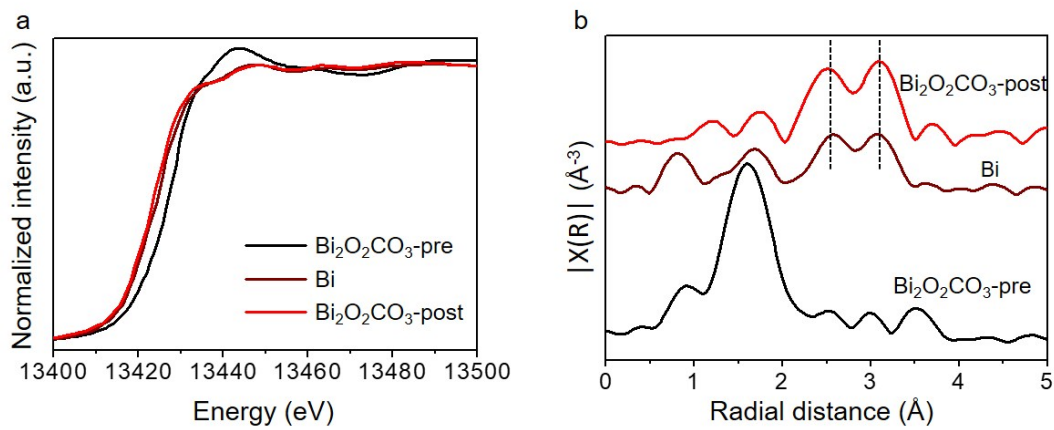


Fig. S9 Bi L₃ edge (a) XANES and (b) EXAFS spectra of commercial Bi powders and Bi₂O₂CO₃ before and after CO₂RR test.

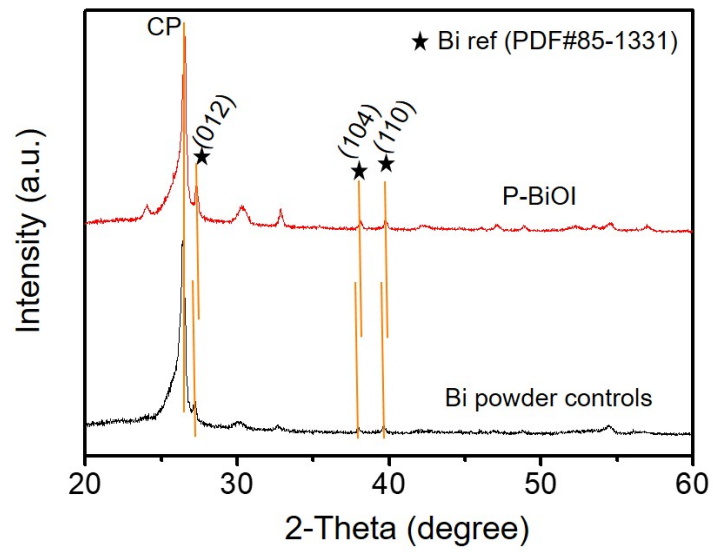


Fig. S10 XRD patterns of P-BiOI and Bi powder controls, both of which were collected at the potential of -1.50 V for 6 h. The extra diffraction peaks of Bi powder controls after CO_2RR were ascribed to $\text{Bi}_2\text{O}_2\text{CO}_3$.

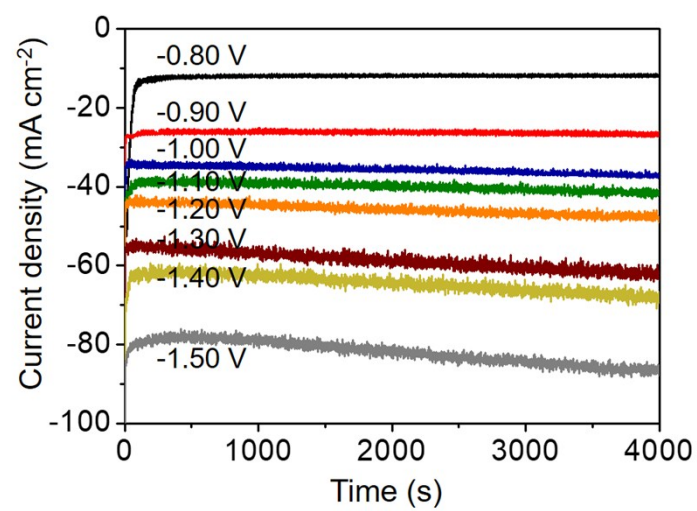


Fig. S11 Chronoamperometric curves of P-BiOI operated at different potentials.

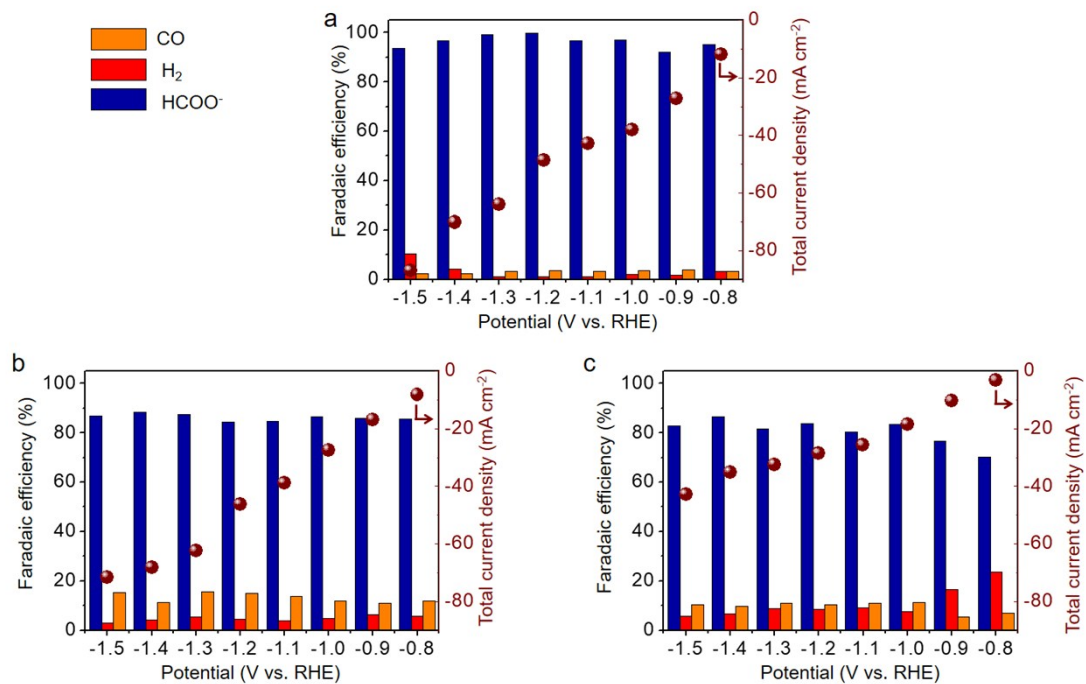


Fig. S12 Potential-dependent Faradaic efficiencies of CO, H₂ and HCOO⁻ along with total current density for (a) P-BiOI, (b) P-Bi₂O₂CO₃ and (c) commercial Bi powders, respectively.

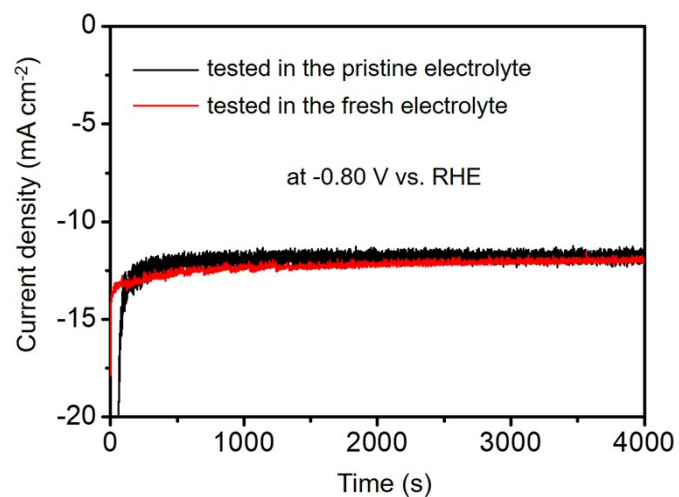


Fig. S13 Chronoamperometric curves of P-BiOI operated at -0.80 V in the pristine electrolyte and fresh electrolyte, respectively.

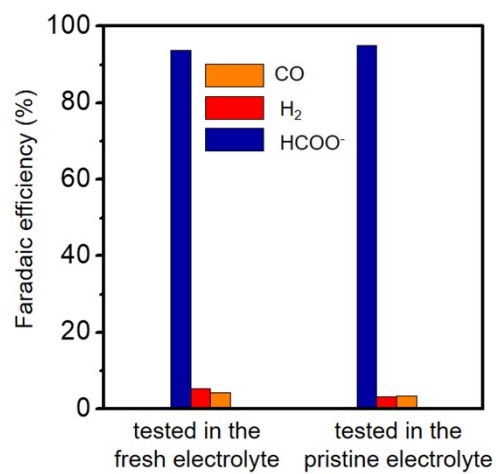


Fig. S14 Faradaic efficiency of P-BiOI tested in the different electrolyte under the potential of -0.80 V.

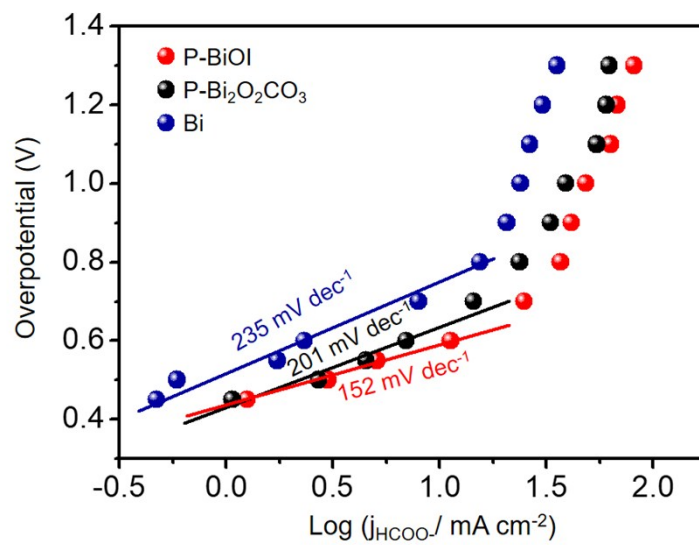


Fig. S15 Partial current density Tafel plots on the P-BiOI, P-Bi₂O₂CO₃ and Bi electrodes.